# Dalton Transactions

Accepted Manuscript

Dynamic Article Links ►

Cite this: DOI: 10.1039/c0xx00000x

www.rsc.org/xxxxxx

ARTICLE TYPE

# Intense Photo- and Tribo-luminescence of Three Tetrahedral Manganese(II) Dihalides with Chelating Bidentate Phosphine Oxide Ligand

**Jun Chen,[a,b] Qing Zhang,[a,b] Fa-Kun Zheng,[*,a] Zhi-Fa Liu,[a] Shuai-Hua Wang,[a] A-Qing Wu,[a] and Guo-Chong Guo[a]**

***Received (in XXX, XXX) Xth XXXXXXXXX 20XX, Accepted Xth XXXXXXXXX 20XX***
**DOI: 10.1039/b000000x**

Three air-stable tetrahedral manganese(II) dihalide complexes [$MnX_2$(DPEPO)] (DPEPO = bis[2-(diphenylphosphino)phenyl]ether oxide; X = Cl, Br and I) were prepared. All of the obtained compounds have been structurally characterized by single-crystal X-ray diffraction analyses, which reveal that they crystallize in centrosymmetry space groups and feature an isolated mononuclear structure with $Mn^{2+}$ in a tetrahedral environment. Interestingly, these complexes show an excellent photoluminescent performance in neat solid with a total quantum yield ($\Phi_{total}$) high up to 70% for the dibromide complex. Simultaneously, intense green flash light could be observed by naked eyes when rubbing the manganese(II) complexes.

## Introduction

Over the past decades, divalent manganese ions have attracted considerable interest as green or red phosphors because of their emissions from the $^4T_1(G)\rightarrow{}^6A_1$ transition which is strongly dependent on the crystal field. Compounds with $Mn^{2+}$ in a tetrahedral environment usually give out green emissions[1-4], while those with octahedrally coordinated $Mn^{2+}$ tend to have orange to red emissions[5-8]. A well-known kind of $Mn^{2+}$ based brilliant green emitters are salt-like compounds constructed by inorganic tetrahalogenomanganate(II) anions and organic cations,[2, 9-11] which might be promising light-emitting materials for use in cathode-ray tubes, fluorescent tubes, X-ray imaging screens and radiation detectors.[11] Besides, the crystals of these compounds with non-centrosymmetric space group show fascinating characteristic triboluminescence[2, 9, 10, 12] and pressure-dependent photoluminescence[1, 13]. However, most of these compounds are easily hydrolyzed by water in air and their emissions are drastically quenched when the temperature raises up to the point (usually bellow 100℃) at which the solid–solid phase transition or melting occurs[2, 10, 11, 14]. Simultaneously, the report about quantum efficiency of these complexes is limited.

Neutral tetrahedral $Mn^{2+}$ complexes $MnX_2(Ph_3PO)_2$ (X = Cl, Br) are obtained through introduction of triphenylphosphine oxide $Ph_3PO$[12, 13, 15, 16]. However, photoluminescence of them are less intense than the ionic ones, and $MnCl_2(Ph_3PO)_2$ is actually non-luminescence. The chelating bidentate phosphine oxide DPEPO (bis[2-(diphenylphosphino)phenyl]ether oxide) can act as a good antenna ligand for an effective intersystem crossing process of $^1\pi\pi^*–^3\pi\pi^*$[17-19], and the energy gaps between $^3\pi\pi^*$ and G-terms of $Mn^{2+}$ are suitable for energy transfer. Meanwhile, the rigidity of DPEPO may prevent non-radiative deactivation pathways. Therefore, the intensity of photoluminescence for these complexes is highly improved compared with the triphenylphosphine oxide analogue complexes. Additionally, compared with $Ph_3PO$, the greater steric bulk of DPEPO more efficiently enhances stability of these complexes. Herein, we first employ DPEPO in synthesizing $Mn^{2+}$ complexes and report three novel tetrahedral $Mn^{2+}$

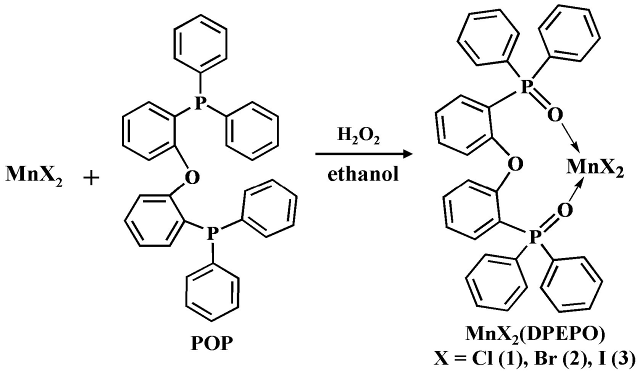

**Scheme 1** The synthetic route for **1–3**

---

a State Key Laboratory of Structural Chemistry, Fujian Institute of Research on the Structure of Matter, Chinese Academy of Sciences, Fuzhou, Fujian 350002, P. R. China. Fax: (+86) 591-8371-4946; Tel:86-591-83704827; E-mail: zfk@fjirsm.ac.cn; b University of Chinese Academy of Sciences, Beijing 100039, P. R. China.

Electronic Supplementary Information (ESI) available: X-ray crystallographic files in CIF format of **1–3**, TL video of **1–3**, selected bond lengths and angles, hydrogen-bonds, thermochemical properties, PXRD patterns, solid-state UV/Vis absorbance spectra, Photoluminescence lifetime data and fitted curve, Photographs of TL, emission spectro for desolvent samples for **1** and **2**, CIE chromaticity diagram and FT-IR spectra. See DOI: 10.1039/c000000x/.

complexes, [MnX$_2$(DPEPO)]·EtOH, (X = Cl for **1**, Br for **2**) and [MnI$_2$(DPEPO)] (**3**), showing air stability, intense green phosphorescence and vivid triboluminescence. The decent quantum efficiency of photoluminescence varying from 32 to 70% and relative long lifetimes ranging from 0.1 to 2.2 ms for **1**–**3** were recorded and discussed.

## Experimental Section

### Materials and Instruments

All chemicals were commercially available, of analytical grade, and used without further purification. The elemental analysis of C and H were determined with a Vario EL III elemental analyzer. The FT-IR spectra were recorded in the 4000–400 cm$^{-1}$ range with a Perkin–Elmer Spectrum One Spectrometer using KBr pellets. The UV/Vis spectra were measured at room temperature using a Perkin-Elmer Lambda 900 UV–vis spectrophotometer equipped with an integrating sphere attachment and BaSO$_4$ as reference. The photoluminescence (PL) and lifetime determination were conducted on a single-grating Edinburgh EI920 fluorescence spectrometer equipped with a 450 W Xe lamp, an μF900 lamp and a PMT detector. The quantum yield was measured on an Edinburgh FLS920 fluorescence spectrometer equipped with a BaSO$_4$-coated integrating sphere, a 450 W Xe lamp and a R928P PMT detector in the single-photon counting mode. Photographs of crystals and photoluminescence, as well as videos of triboluminescence for **1**–**3**, were recorded by digital camera Canon IXUS 105. Thermogravimetric analysis (TGA) experiments were done on a NETZSCH STA 449C Jupiter thermogravimetric analyzer in flowing nitrogen with the sample heated in an Al$_2$O$_3$ crucible at a heating rate of 10 Kmin$^{-1}$. All powdered X-ray diffraction data were collected on a Rigaku Miniflex II diffractometer using Cu-K$\alpha$ radiation ($\lambda$ = 1.540598 Å) at 40 kV and 40 mA in the range 5.00° ≤ 2$\theta$ ≤ 65.00°.

### Syntheses of 1–3

**[MnCl$_2$(DPEPO)]·EtOH (1).** A mixture of POP (0.2 mmol, 106 mg) and anhydrous MnCl$_2$ (0.4 mmol, 0.050 g) was solved in ethanol (6 mL), and 0.1mL H$_2$O$_2$ (30%) was added. The mixture was stirred for 1h at room temperature and transferred to a 25 mL Teflon-lined stainless-steel autoclave heated at 120 °C for 1 day, and then naturally cooled to room temperature. The reaction mixture was filtered and stood in diethyl ether atmosphere at room temperature for several days. Light green block crystals of **1** suitable for X-ray analyses were obtained, washed with diethyl ether and dried in air. Yield: 55% (based on POP) for **1**. Anal. Calcd for C$_{38}$H$_{34}$Cl$_2$MnO$_4$P$_2$: C, 61.48; H, 4.61. Found: C, 61.40; H, 4.62. IR (KBr pellet, cm$^{-1}$): 3470 m br, 3057 w, 2963 w, 2920 w, 1591 w, 1568 w, 1462 m, 1437 s, 1267 m, 1225 s, 1177 s, 1134 m, 1121 m, 1103 w, 1078 w, 997 w, 878 w, 802 w, 752 m, 752 m, 731 m, 694 m, 584 w, 546 s, 519 w, 436 w.

**[MnBr$_2$(DPEPO)]·EtOH (2).** The procedure was similar to that for **1** except that MnCl$_2$ was replaced by MnBr$_2$·4H$_2$O (0.4 mmol, 0.115 g). Green block crystals of **2** suitable for X-ray analyses were directly obtained after opening the Teflon-lined stainless-steel autoclave, washed with diethyl ether and dried in air. Yield: 76% (based on POP) for **2**. Anal. Calcd for C$_{38}$H$_{34}$Br$_2$MnO$_4$P$_2$: C, 54.90; H, 4.12. Found: C, 54.80; H, 4.15. IR (KBr pellet, cm$^{-1}$): 3487 m br, 3057 w, 2924 w, 1591 w, 1568 w, 1462 m, 1437 s, 1267 m, 1229 s, 1175 s, 1134 m, 1120 m, 1103 w, 1078 w, 997 w, 880 w, 800 w, 752 m, 731 m, 714 s, 694 m, 584 w, 548 s, 519 w, 436w.

**[MnI$_2$(DPEPO)] (3).** The procedure was the same as that for **2** except that MnBr$_2$·2H$_2$O was replaced by anhydrous MnI$_2$ (0.4 mmol, 0.124 g). Yellow-green block crystals of **3** suitable for X-ray analyses were obtained, washed with diethyl ether and dried in air. Yield: 42% (based on POP) for **3**. Anal. Calcd for C$_{36}$H$_{28}$I$_2$MnO$_3$P$_2$: C, 49.18; H, 3.21. Found: C, 49.13; H, 3.26. IR (KBr pellet, cm$^{-1}$): 3468 m br, 3057 w, 2922 w, 2850 w, 1591 w, 1568 w, 1462 m, 1439 s, 1267 m, 1238 s, 1180 s, 1163 m, 1134 m, 1123 m, 1105 w, 1080 w, 1028 w, 997 w, 883 w, 800 w, 754 w, 731 m, 712 m, 694 m, 584 w, 548 s, 517 m, 420 w.

### Single crystal structure determination

Single crystals of **1**–**3** suitable for X-ray analyses were stuck to a glass fibre. Data collections were performed on a Rigaku Saturn-70 CCD diffractometer for **1**–**3** at 293 K. The diffractometer was equipped with graphite-monochromated Mo-K$\alpha$ radiation ($\lambda$ = 0.71073 Å). The intensity data sets were collected with the $\omega$ scan technique and reduced by CrystalClear software.[20] The structures were solved by direct methods with the SHELXTL (version 5) crystallographic software package[21] and refined by full-matrix least-squares refinement on $F^2$. Non-hydrogen atoms were located by difference Fourier maps and subjected to anisotropic refinement. The hydrogen atoms were added according to theoretical models. Pertinent crystal data and structure refinement results for **1**–**3** are summarized in Table 1, and selected bonds lengths and angles are listed in Table S1.

**Table1** Crystallographic data and Structural Refinements for **1**–**3**

| | **1** | **2** | **3** |
|---|---|---|---|
| Formula | C$_{38}$H$_{34}$Cl$_2$MnO$_4$P$_2$ | C$_{38}$H$_{34}$Br$_2$MnO$_4$P$_2$ | C$_{36}$H$_{28}$I$_2$MnO$_3$P$_2$ |
| $M_r$ (g mol$^{-1}$) | 742.43 | 831.33 | 879.26 |
| Space group | $P$-1 | $P$-1 | $P2_1$/n |
| $a$/Å | 9.623(4) | 9.717(5) | 12.244(6) |
| $b$/Å | 12.807(5) | 12.898(6) | 16.451(7) |
| $c$/Å | 15.196(6) | 15.304(7) | 18.121(9) |
| $\alpha$/° | 107.779(6) | 107.441(7) | 90 |
| $\beta$/° | 90.856(5) | 91.153(4) | 102.496(11) |
| $\gamma$/° | 93.551(4) | 94.176(4) | 90 |
| $V$/Å$^3$ | 1778.8(12) | 1823.2(15) | 3564(3) |
| $Z$ | 2 | 2 | 4 |
| $D_c$/g cm$^{-3}$ | 1.386 | 1.514 | 1.639 |
| $\mu$/mm$^{-1}$ | 0.650 | 2.680 | 2.226 |
| $F$(000) | 766.0 | 838.0 | 1716.0 |
| total reflns | 12736 | 11918 | 30151 |
| unique reflns | 6013 | 6323 | 8122 |
| $R_{int}$ | 0.0299 | 0.0323 | 0.0308 |
| GOF | 1.025 | 1.009 | 0.996 |
| $R_1$ $^a$[$I$ >2σ($I$)] | 0.0434 | 0.0556 | 0.0275 |
| $wR_2$ $^b$(all data) | 0.1627 | 0.1981 | 0.0708 |
| $CCDC$ | 1030848 | 1030849 | 1030850 |

[a] $R_1 = \sum(F_o - F_c) / \sum F_o$; [b] $wR_2 = [\sum w(F_o^2 - F_c^2)^2 / \sum w(F_o^2)^2]^{1/2}$.

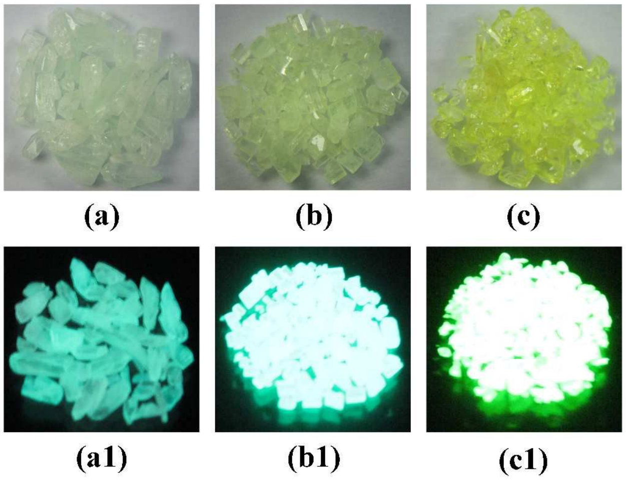

**Fig. 1** Photographs of crystals of **1**–**3** (a for **1**, b for **2** and c for **3**) under ambient light and (a1 for **1**, b1 for **2** and c1 for **3**) under a 365 nm UV light.

## Results and Discussions

### Syntheses and Thermal Stability

Bis(2-(diphenylphosphino)phenyl) ether (POP) can be oxidized to DPEPO by $O_2$ in presence of $MnX_2$ in ethanol. Several drops of $H_2O_2$ added in the mixture of $MnX_2$ and POP will highly improve the yield of **1**–**3**, which may be ascribed to the evidence that the amount of dissolved oxygen in solution is increased by Mn(II) catalyzing $H_2O_2$ decomposition into $H_2O$ and $O_2$.[22, 23] Crystals **1**–**3** are stable in air, which were found to remain unchanged for more than one year. The greenish emission from these compounds (Figure 1) indicates the $Mn^{2+}$ ions are in a tetrahedral environment.[2, 16] Thermogravimetric analyses (TGA) curves (Figure S1) show that the weight loss of 6.11% from 130 to 300 °C in **1** corresponds to the release of one ethanol molecule (calcd: 6.21%). With continuous heating to 380 °C, complex **1** began to decompose. For **2**, the TGA cuver is similar with **1**. The weight loss of 5.57% from 160 to 216 °C is in accordance with the release of one ethanol molecule (calcd: 5.54%). With further heating to 418 °C, complex **2** started to decompose. There is no obvious weight loss before 430 °C for complex **3**. Upon further heating, **3** began to break down. The experimental PXRD patterns of **1**–**3** agree well with the simulated ones based on the single-crystal X-ray data (Figure S2), which implies that **1**–**3** are in a pure phase.

### Structural descriptions

The single-crystal X-ray diffraction analyses reveal that complexes **1**–**3** all crystallize in centrosymmetric space groups (Table 1). Both **1** and **2** are allomeric with an isolated mononuclear structure and crystallize in triclinic space group *P*-1. In each asymmetric unit of **1** and **2**, there is one Mn(II) center, one oganic ligand DPEPO, two halogen ions (Cl in **1**, Br in **2**) and one ethanol lattice molecule (Figures 2a and 2b). Every Mn(II) atom in **1** and **2** is four-coordinated by two oxygen atoms (O1, O2) from one chelating DPEPO ligand and two Cl (or Br) anions. The coordination geometry around the Mn(II) atom can be described as a distorted tetrahedron with the angles varying from 105.53(8) to 112.60(4)° in **1** and 105.43(13) to 112.78(11)° in **2**. The bond distances of Mn–O in **1** (2.0327(19)–2.0498(19) Å) and **2** (2.017(3)–2.049(3) Å) fall in the similar range, while the bond lengths of Mn–Cl (2.3230(10)–2.3425(13) Å) in **1** are slightly shorter than those of Mn-Br (2.4687(11)–2.4876(14) Å) in **2**, which arises from the fact that the radius of Cl ion is smaller than that of Br ion. The exsistence of hydrogen bonds X···H–O between the host mononuclear Mn(II) unit and guest ethanol molecule (Table S2, Cl in **1**, Br in **2**) further stabilizes the crystal structure. Compound **3** crystallizes in monoclinic space group $P2_1/n$. The mononuclear structure of **3** (Figure 2c) is similar to those of **1** and **2**, but the packing is different from that of **1** and **2**. There is not any solvent molecule in **3**, which is also checked by PLATON software.[24] The selected bond distances and angles for **1**–**3** are listed in Table S1.

### Electronic Spectroscopy

For tetrahedrally coordinated $Mn^{2+}$, the expected intraconfigurational electron transitions including two distinct groups (D-terms and G-terms) of absorption bands are assigned to the range 300–500 nm[1, 2, 25, 26]. In general, the bands of the D-terms appear with stronger intensities than those of the G-terms. As displayed in Figure S3, **1**–**3** show similar absorption wavelengths but different intensities. The intense absorption bands *ca.* 320 nm and 369 nm in the UV/Vis region belong to the transitions from $^6A_1$ ground term to the $^4E(D)$ and $^4T_2(D)$ terms, respectively. The intensity relating to $^6A_1 \rightarrow ^4E(D)$ transition in **1** is much weaker than in **2** and **3**, which may be the consequence of different ligand field strength of the halogen anions. The other relatively weak bands located at *ca.* 423 nm, 440 nm and 463 nm correspond to the transitions to

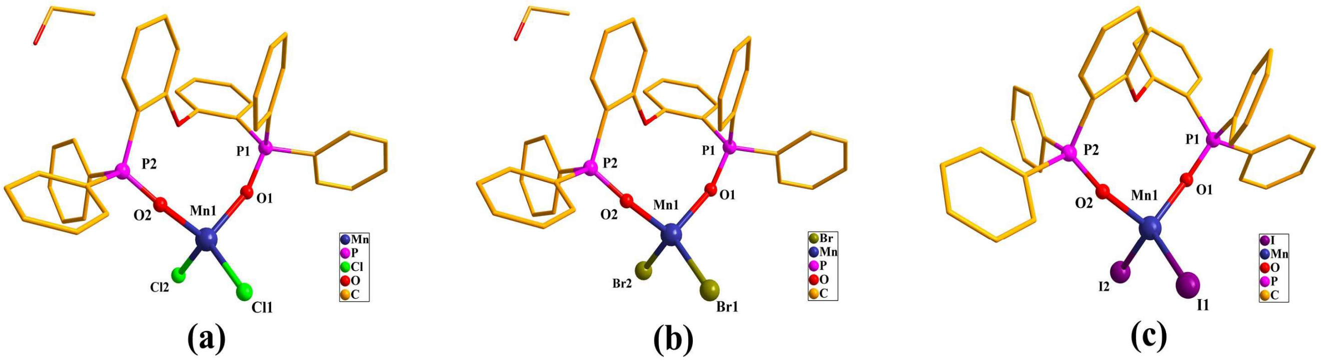

**Fig. 2** Molecular structures of **1**(a), **2**(b) and **3**(c). Hydrogen atoms have been omitted for clarity

Cite this: DOI: 10.1039/c0xx00000x

www.rsc.org/xxxxxx

**Table 2** Photophysical Parameters for **1**–**3** in the solid state under 298K

| Complexes | $\lambda_{em}$ (nm) | $\tau$ (ms)$^a$ | $\Phi_{total}{}^b$ (%) |
|---|---|---|---|
| **1** | 507 | 2.2 | 32 |
| **2** | 502 | 0.5 | 70 |
| **3** | 528 | 0.1 | 64 |
| **$MnBr_2(Ph_3PO)_2$** | 518 | 0.1 | 23 |

$^a$ Fitted by single-exponential. $^b$ Error ±2%.

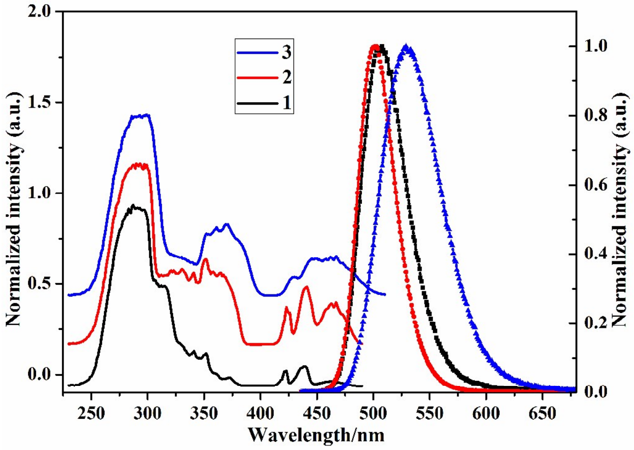

**Fig. 3** Solid-state excitation spectra (left, $\lambda_{em}$ = 507, 502, 528 nm for **1**–**3**, respectively) and emission spectra (right) of **1**–**3** measured at 298K ($\lambda_{ex}$ = 303 nm).

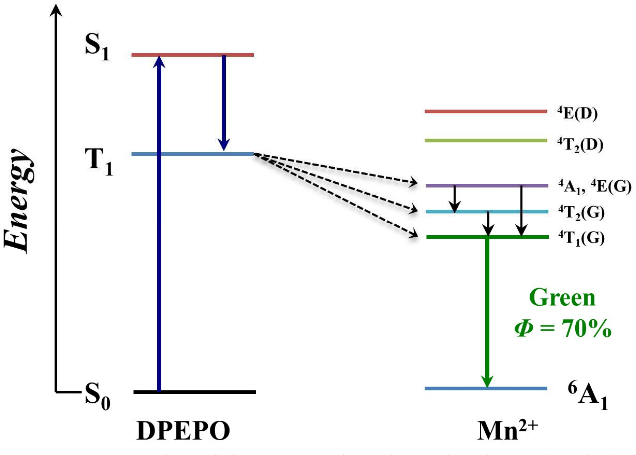

**Fig. 4** Representation of the energy adsorption, migration and emission process of the Mn(II) complexes. The highest quantum yield $\Phi$ = 70 % is for **2**.

G-terms $^6A_1\rightarrow^4A_1$, $^4E(G)$, $^6A_1\rightarrow^4T_2(G)$ and $^6A_1\rightarrow^4T_1(G)$, respectively, which can be clearly observed in **2**. Besides, the one more intense band at 295 nm is in consistent with the transition of $\pi\pi$–$^1\pi\pi$* of DPEPO, which shows that the organic ligand DPEPO acting as antenna can effectively absorb energies from UV-radiation. The profiles of excitation spectra (Figure 3) are in agreement with those of UV/Vis spectra, and the maximum excitation bands of these complexes are all relative to $\pi\pi$–$^1\pi\pi$* transition of DPEPO. The fact further confirms DPEPO is a highly efficient sensitizer for tetrahedral Mn(II) luminescence.

### Photophysical Properties

The photoluminescent properties of **1**–**3** are presented in Table 2. The emission peaks at room temperature are broad and correspond to the characteristic $^4T_1(G)\rightarrow^6A_1$ radiative transition (Figure 3). Complexes **1** and **2** display green emissions located at 507 and 502 nm, respectively, and complex **3** gives a yellow-greenish emission centred at 528 nm. The bathochromic shift in emission for **3** may be ascribed to the lower ligand field strength of $I^-$. The decay curves of $^4T_1(G)\rightarrow^6A_1$ radiative transition for these complexes are fitted by a single exponential function (Figures S4–S6), indicating that just one optical $Mn^{2+}$ species was present. The emission decay times of **1**–**3** are 2.2 ms, 0.5 ms and 0.1 ms, respectively**,** dramatically decreasing from Cl to Br to I. This phenomenon can be interpreted by heavy atom effects.[14] With the nuclear charge number increasing from Cl to Br to I, the spin-orbit coupling interactions in **1**–**3** become larger and hence lead to a reduction in the lifetime of the excited state. However, the phosphorescence intensity tends to increase. Solid state of complex **1** has a moderate quantum efficiency of 32%, while complexes **2** and **3** glow brightly with emission efficiencies up to 70 and 64%, respectively. We also measured the photoluminescence quantum efficiency of the reported analogue complex $MnBr_2(Ph_3PO)_2$[9, 13] with a much lower quantum efficiency of 23% than its corresponding DPEPO complex **2**, which is most likely due to the greater flexibility of $Ph_3PO$ providing more non-radiative decay pathways.

Reinhoudt's empirical rule[27] points out that the intersystem crossing process becomes effective when energy gap ΔE ($^1\pi\pi^*$–$^3\pi\pi^*$) is ≥ 5000 $cm^{-1}$. The energy gap for DPEPO is 6620 $cm^{-1}$, hence the intersystem crossing is effective for DPEPO.[17, 18] The singlet energy levels of DPEPO ($^1\pi\pi^*$ = 32258 $cm^{-1}$) and the energy states of $Mn^{2+}$ ion were estimated from the onset wavelength of the absorption spectra of **1**–**3**, and the energy of the triplet level of DPEPO (25638 $cm^{-1}$) was found to be higher than that of the $^4A_1$, $^4E(G)$ state (23256 $cm^{-1}$) of $Mn^{2+}$. Therefore, energy can be effectively transferred to $Mn^{2+}$ ion. The possible energy migration pathway is shown in Figure 4. DPEPO is excited by absorption of ultraviolet light to singlet state $^1\pi\pi^*$, and energy migration via non-radiative intersystem crossing from the singlet $^1\pi\pi^*$ to the triplet state $^3\pi\pi^*$, then the triplet energy transfers to the G-terms of $Mn^{2+}$ ion, which are thermally quenched to $^4T_1$ state. Finally, $^4T_1$ state undergoes radiative decay to the ground state leading to the observed luminescence.

### Triboluminescence Properties

Triboluminescence (TL) caused by mechanical energy applied to a material has generated extensive research interest over the years, [15, 28-32] because of its potential application for real-time sensors of mechanical stress, structural damage, and a resource of X-ray emssion. Jeffrey L. Zink had elaborated comprehensively the origin of excitation process caused by rubbing the TL materials[13, 33]. Nevertheless, so far, the underlying mechanism for the process is still unclear. A widely-accepted opinion holds that charges separated during fracture results in triboluminescence.[34, 35] Previous studies supported that only piezoelectric (non-centrosymmetric) crystals may be responsible for triboluminescent since only such crystals can develop opposite charges on the opposing faces of a developing crack. However, several reports of centrosymmetric triboluminescent materials cast doubt on that assumption.[28, 34, 36] Two rational explanations about why the centrosymmetric crystals display TL properties have been developed: one was proposed by Rheingold[37] that ionic compounds may permit charge separation by partial fracture along planes with opposite charges, and the other one was proposed by Sweeting[34] that the disorder groups may provide a sufficient source of localized polarity to produce charge separation upon cleavage. The known crystal structures of $Mn^{2+}$ complexes showing TL are all non-centrosymmetrical[9, 13]. However, the intensely triboluminescent compounds **1**–**3** presented here are centrosymmetric and non-ionic, and no disordered groups in them were found during structure refinement. Thus the mechanism for TL in these compounds must be different from these two previously-proposed mechanisms. Since the greenish colour of TL for **1**–**3** (Figure S7 and TL vedio) is similar with PL, the TL can be assigned to the same $^4T_1(G)\rightarrow{}^6A_1$ transition as PL[13, 33]. Besides, the search for TL material with intense emission is very important for inexpensive and compact detectors. Bourhill suggested that TL efficiency could be improved by increasing the PL quantum yield[38]. Hence, a high PL quantum yield is desirable to obtain intense TL, and that is what we have demonstrated with these compounds.

## Conclusion

In this work, we report three novel tetrahedral manganese(II) dihalide complexes with a bidentate phosphine oxide ligand showing high photoluminescence quantum yields and long excited state lifetimes. The quantum yield for complex **2** is up to 70% and the life time is 0.5 ms at room temperature. The optical properties analysis suggests that a combination of the heavy atom effect and differing ligand-field properties associated with variation in the halide ligands account for the observed photophysical properties. Additionally, the introduction of the double chelating ligand DPEPO not only increases the stability of the Mn(II) compounds, but also acts as an antenna for sensitized Mn(II) luminescence. The increased stability, enhanced intensity and long life time ensure the obtained compounds **1**–**3** being excellent green phosphors potential applications in industry. Furthermore, the crystals of **1**–**3**, displaying fascinating intense flash light when being rubbed, represent first centrosymmetric tetrahedral manganese(II) triboluminescent examples. The centrosymmetric space groups, non-ionic structures and the lack of disorder group for complexes **1**–**3** exclude the mentioned mechanisms for triboluminescence, and the search for a rational explanation is still on the way.

## Acknowledgements

This work was financially supported by 973 Program (2011CBA00505) and National Nature Science Foundation of China (21371170 and 21103188).

## References

1. Y. Rodríguez-Lazcano, L. Nataf and F. Rodríguez, *Phys. Rev. B*, 2009, **80**, 085115-1.
2. S. Pitula and A. V. Mudring, *Chem. Eur. J.*, 2010, **16**, 3355.
3. K. N. Kim, H. K. Jung, H. D. Park and D. Kim, *J. Lumin.*, 2002, **99**, 169.
4. S. R. Lukić, D. M. Petrović, M. D. Dramićanin, M. Mitrić and L. Đačanin, *Scripta Mater.*, 2008, **58**, 655.
5. J. Orive, J. L. Mesa, R. Balda, J. Fernández, J. R. Fernández, T. Rojo and M. I. Arriortua, *Inorg. Chem.*, 2011, **50**, 12463.
6. J. Lin, Q. Zhang, L. Wang, X. C. Liu, W. B. Yan, T. Wu, X. H. Bu and P. Y. Feng, *J. Am. Chem. Soc.*, 2014, **136**, 4769.
7. Z. T. Deng, L. Tong, M. Flores, S. Lin, J. X. Cheng, H. Yan and Y. Liu, *J. Am. Chem. Soc.*, 2011, **133**, 5389.
8. O. Chen, D. E. Shelby, Y. Yang, J. Zhuang, T. Wang, C. Niu, N. Omenetto and Y. C. Cao, *Angew. Chem., Int. Ed.*, 2010, **49**, 10132.
9. F. A. Cotton, L. M. Daniels and P. Huang, *Inorg. Chem.*, 2001, **40**, 3576.
10. S. Balsamy, P. Natarajan, R. Vedalakshmi and S. Muralidharan, *Inorg. Chem.*, 2014, **53**, 6054.
11. K. Seddon, M. Earle, WO2006043110 (A1), United Kingdom, 2006.
12. B. P. Chandra, M. S. K. Khokhar, R. S. Gupta and B. Majumdar, *Pramna-J. Phys.*, 1987, **29**, 399.
13. G. E. Hardy and J. I. Zink, *Inorg. Chem.*, 1976, **15**, 3061.
14. N. Presser, M. A. Ratner and B. R. Sundheim, *Chem. Phys.*, 1978, **31**, 281.
15. B. P. Chandra, *J. Lumin.*, 1982, **27**, 101.
16. D. M. L. Goodgame and F. A. Cotton, *J. Chem. Soc. (Resumed)*, 1961, 3735.
17. S. Biju, N. Gopakumar, J. C. G. Bunzli, R. Scopelliti, H. K. Kim and M. L. P. Reddy, *Inorg. Chem.*, 2013, **52**, 8750.
18. S. Biju, M. L. P. Reddy, A. H. Cowley and K. V. Vasudevan, *Cryst. Growth Des.*, 2009, **9**, 3562.
19. O. Moudam, B. C. Rowan, M. Alamiry, P. Richardson, B. S. Richards, A. C. Jones and N. Robertson, *Chem. Commun.*, 2009, **43**, 6649.
20. CrystalClear, version 1.35; Software User's Guide for the Rigaku R-Axis and Mercury and Jupiter CCD Automated X-ray Imaging System; Rigaku Molecular Structure Corporation: UT, 2002.
21. SHELXTL Reference Manual, version 5; Siemens Energy & Automation Inc.: Madison, WI, 1994.
22. P. J. Pessiki, S. V. Khangulov, D. M. Ho and G. C. Dismukes, *J. Am. Chem. Soc.*, 1994, **116**, 891.
23. V. V. Barynin, M. M. Whittaker, S. V. Antonyuk, V. S. Lamzin, P. M. Harrison, P. J. Artymiuk and J. W. Whittaker, *Structure*, 2001, **9**, 725.

24. A. L. Spek, *PLATON, A Multipurpose Crystallographic Tool*, 2005.
25. C. Furlani and A. Furlani, *J. Inorg. Nucl. Chem.*, 1961, **19**, 51.
27. F. J. Steemers, W. Verboom, D. N. Reinhoudt, E. B. Van der Tol and J. W. Verhoeven, *J. Am. Chem. Soc.*, 1995, **117**, 9408.
28. X. F. Chen, C. Y. Duan, X. H. Zhu, X. Z. You, S. S. S. Raj, H. K. Fun and J. Wu, *Mater. Chem. Phys.*, 2001, **72**, 11.
29. L. M. Sweeting, *Chem. Mater.*, 2001, **13**, 854.
30. C. G. Camara, J. V. Escobar, J. R. Hird and S. J. Putterman, *Nature*, 2008, **455**, 1089.
31. T. D. David, O. Olawale, W. G. Sullivan , O. I. Okoli, J. O. Sobanjo and B. Wang, *J. Lumin.*, 2011, **131**, 1407
32. P. Jha and B. P. Chandra, *Luminescence*, 2014, DOI: 10.1002/bio.2647.
33. J. I. Zink, *Acc. Chem. Res.*, 1978, **11**, 289.
34. L. M. Sweeting and A. L. Rheingold, *J. Am. Chem. Soc.*, 1987, **109**, 2652.
35. J. T. Dickinson, L. B. Brix and L. C. Jensen, *J. Phys. Chem.*, 1984, **88**, 1698.
36. X. F. Chen, X. H. Zhu, Y. H. Xu, S. S. S. Raj, S. Ozturk, H. K. Fun, J. Ma and X. Z. You, *J. Mater. Chem.*, 1999, **9**, 2919.
37. A. L. Rheingold and W. King, *Inorg. Chem.*, 1989, **28**, 1715.
38. G. Bourhill, L. O. Pålsson, I. D. W. Samuel, I. C. Sage, I. D. H. Oswald and J. P. Duignan, *Chem. Phys. Lett.*, 2001, **336**, 234.

# Graphical Abstract

## Intense Photo- and Tribo-luminescence of Three Tetrahedral Manganese(II) Dihalides with Chelating Bidentate Phosphine Oxide Ligand

Jun Chen,[a,b] Qing Zhang,[a,b] Fa-Kun Zheng,[*,a] Zhi-Fa Liu,[a] Shuai-Hua Wang,[a] A-Qing Wu,[a] and Guo-Cong Guo[a]

[a] *State Key Laboratory of Structural Chemistry, Fujian Institute of Research on the Structure of Matter, Chinese Academy of Sciences, Fuzhou, Fujian 350002, P. R. China;* [b] *University of Chinese Academy of Sciences, Beijing 100039, P. R. China*

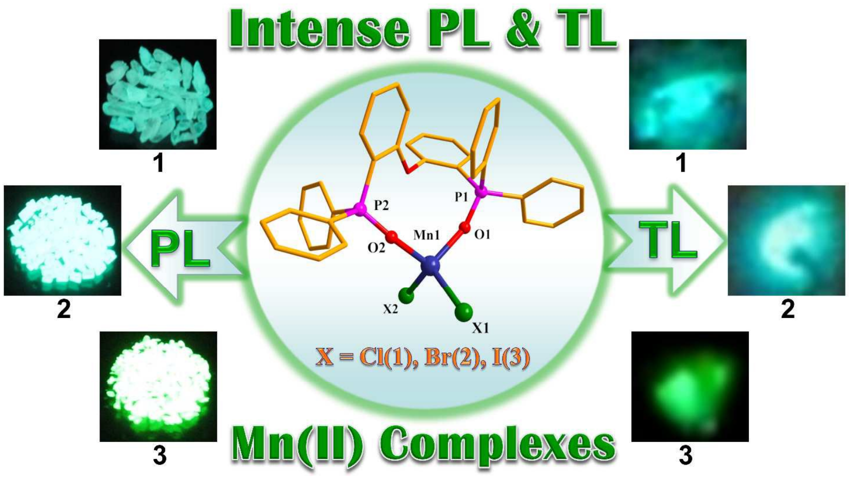

Three air-stable centrosymmetric tetrahedral manganese(II) dihalide complexes with chelating bidentate phosphine oxide ligand show a high emission efficiency with a total quantum yield varying from 32 to 70% and relative long lifetimes ranging from 0.1 to 2.2 ms.

---

[*] Corresponding author. Tel: +86 591 83704827; fax: +86 591 83714946.

E-mail address: zfk@fjirsm.ac.cn (F.-K. Zheng).

Moreover, these complexes, displaying intense flash light when being rubbed, represent first centrosymmetric tetrahedral manganese(II) triboluminescent examples.